

Growth of Neurites toward Neurite–Neurite Contact Sites Increases Synaptic Clustering and Secretion and Is Regulated by Synaptic Activity

Joshua Cove^{1,2,3,*}, Pablo Blinder^{1,2,3,*}, Elia Abi-Jaoude^{4,*},
Myriam Lafrenière-Roula⁵, Luc Devroye⁶ and
Danny Baranes^{1,2,3}

¹Department of Life Sciences, Ben-Gurion University of the Negev, Beer-Sheva 84105, Israel, ²The National Institute for Biotechnology in the Negev, Ben-Gurion University of the Negev, Beer-Sheva 84105, Israel, ³Zlotowsky Center for Neuroscience, Ben-Gurion University of the Negev, Beer-Sheva 84105, Israel, ⁴Department of Psychiatry, University of Toronto, Toronto, Ontario, Canada M5T 1R8, ⁵Spinal Cord Research Centre, University of Manitoba, Winnipeg, Manitoba, Canada R3E 3J7 and ⁶School of Computer Science, McGill University, Montreal, Canada H3A 2K6

*These authors contributed equally to this work.

The integrative properties of dendrites are determined by several factors, including their morphology and the spatio-temporal patterning of their synaptic inputs. One of the great challenges is to discover the interdependency of these two factors and the mechanisms which sculpt dendrites' fine morphological details. We found a novel form of neurite growth behavior in neuronal cultures of the hippocampus and cortex, when axons and dendrites grew directly toward neurite–neurite contact sites and crossed them, forming multi-neurite intersections (MNIs). MNIs were found at a frequency higher than obtained by computer simulations of randomly distributed dendrites, involved many of the dendrites and were stable for days. They were formed specifically by neurites originating from different neurons and were extremely rare among neurites of individual neurons or among astrocytic processes. Axonal terminals were clustered at MNIs and exhibited higher synaptophysin content and release capability than in those located elsewhere. MNI formation, as well as enhancement of axonal terminal clustering and secretion at MNIs, was disrupted by inhibitors of synaptic activity. Thus, convergence of axons and dendrites to form MNIs is a non-random activity-regulated wiring behavior which shapes dendritic trees and affects the location, clustering level and strength of their presynaptic inputs.

Keywords: dendritic morphology, neurite–neurite contact, synaptic clustering, synaptic secretion

Introduction

The morphology of dendritic trees and the distribution of synaptic connections along these trees influence the way neurons receive and process information (Mel, 1993; Schiller *et al.*, 2000; Scott and Luo, 2001; Krichmar *et al.*, 2002). However, what determines the fine details of dendritic and axonal morphology is an open question. Neuritic morphogenesis involves both intrinsic and extrinsic control of branching, growth, and stabilization (Koester and O'Leary, 1992; Threadgill *et al.*, 1997; Kim and Chiba, 2004). However, extrinsic controls, like guiding molecules and growth factors, are diffuse and have a global effect on neurite growth (Kim and Chiba, 2004). Contact-mediated guidance allows for a more localized control of neurite growth. For instance, interneuronal contacts can lead to altered rates of neurite extension (Van den Pol, 1980; Fletcher *et al.*, 1994; Sang and Tan, 2003) via contact-induced signaling of surface molecules like the Eph receptors and their ligands (Orioli and Klein, 1997), or of intracellular molecules

such as Notch (Sestan *et al.*, 1999) and Slit (Whitford *et al.*, 2002). Hence, the interaction of neurons with their neighbours is a key factor in determining the final shape of their neurites.

Cell–cell contact provides a more local control over neurite morphology, when it occurs between neurites. Recent findings showed that neurite–neurite contacts are structurally and functionally distinctive structures. Clusters of the adhesion molecule N-CAM are immobilized at neurite intersections, trapping trans-Golgi network vesicles by binding to spectrin (Sytnyk *et al.*, 2002). These exocytotic vesicles could release signaling molecules to locally affect neurite outgrowth. Hence, contacts made by neurites with their neighbours should be included in the morphological analysis and will most likely yield new insights about organization of both single and ensembles of neurites. This idea has been applied by groups describing neuronal networks in terms of neurite–neurite contact sites connected by neurites (Shefi *et al.*, 2002; da F. Costa *et al.*, 2004). Using this approach, Shefi *et al.* (2002) found that neurites of grasshopper ganglion cells in culture self-organized into 'small world networks' (Watts and Strogatz, 1998). This type of organization is also prominent in the hippocampus and is, in theory, responsible for economical wiring (Buzsaki *et al.*, 2004) and formation of specific network activity patterns (Lago-Fernandes *et al.*, 2000). Hence, physical neurite–neurite contacts play a key role in shaping individual and ensembles of neurites.

Neurite–neurite contact-dependent growth has direct implications to the physiology of neuronal networks. If neurite–neurite contacts enhance neuritic growth, we could expect a clustered distribution of neurites, and hence of their synaptic connections, in the network. Clustered synapses have a strong influence on dendritic integration since they differ from diffused ones in their firing amplitude (Liu and Tsien, 1995), and their sigmoid rather than linear summation (Polsky *et al.*, 2004). Clusters of synaptic connections exist in hippocampal cultures and are formed in an activity-dependent manner (Kavalali *et al.*, 1999). However, a relation between synaptic cluster formation and the morphogenesis of dendrites and axons has not been demonstrated.

We show here for the first time that both axons and dendrites of hippocampal and cortical neurons in culture grow directly toward neurite–neurite intersections in an activity-regulated manner, forming intersections composed of three or more neurites. These multi-neurite intersections bear clusters of axonal terminals with higher synaptophysin content and release

capability compared with axonal terminals elsewhere. Hence, neurite convergence into multi-neurite intersections is a new type of neurite behavior that shapes the wiring morphology of a neuronal network and links it to the distribution and strength of the presynaptic sites.

Materials and Methods

Cell Culture and Treatment

Either hippocampal CA3 and dentate gyrus regions or the anterior half of the cerebral cortex from both hemispheres were dissected out from the brains 1- to 4-day-old Sprague-Dawley rat pups. The tissue was treated for 30 min at 37°C with 0.25% trypsin (Sigma, type XI), dissociated gently and plated at a concentration of 2×10^5 cells/ml (hippocampus) or 3×10^5 cells/ml (cortex) onto 12 mm glass cover slips coated with poly-D-lysine (Sigma, 20 µg/ml) and laminin (Collaborative Research, 10 µg/ml), as described previously (Baranes *et al.*, 1996). Briefly, cells were plated in MEM (Sigma) containing 10% heat inactivated normal goat serum, 1% L-glutamine and 0.8% D-glucose. One day after plating, cells were transferred to serum-free medium containing 45% MEM, 40% DMEM, 10% F12, 0.25% (w/v) BSA, 1% DiPorzio supplement, 0.75% of 45% D-glucose, 0.5% B27 supplement, 0.25% L-glutamine, 0.01% kinurenic acid, 0.01% of mixed 70% uridine and 30% fluoro-deoxyuridine. These cultures were maintained for up to 3 weeks in an incubator at 37°C in a 5% CO₂ atmosphere in the presence or absence of 10 µM 6-cyano-7-nitroquinoxaline-2,3-dione (CNQX), 50 µM 2-amino-5-phosphopentanoic acid (AP-5) or 1 µM tetrodotoxin (TTX).

Immunocytochemistry

For the immunocytochemistry study, cells were labeled as described previously (Baranes *et al.*, 1998). Briefly, cells were fixed for 10 min at room temperature with 4% paraformaldehyde, permeabilized with 0.25% Triton and blocked with 3% normal goat serum. The cells were then incubated overnight at 4°C with anti-microtubule associated protein 2 (MAP2) (1 µg/ml) (monoclonal, Sigma, Oakville, Ontario, Canada), anti-neurofilament M (NFM) (0.5 µg/ml) (polyclonal, Chemicon, Temecula, CA), anti-synaptophysin (0.5 µg/ml) (polyclonal, DAKO, Mississauga, Ontario, Canada) and glial fibrillary acidic protein (GFAP, polyclonal, DAKO) antibodies. The immunolabeling was visualized with secondary antibodies conjugated to Alexa-488 or Cy3 (2 µg/ml) (Molecular Probes, Eugene, OR).

Light Microscopy

Images were obtained on Zeiss Axiovert S-100 and Axiovert 200M microscopes with Plan-Neofluar 20X/0.5 and Plan-Apochrome 63X/1.4 objectives, equipped with 12 MHz CCD cameras (DVC 1300, DVC Company, Austin, TX and SensiCam, PCO, Kolheim, Germany) and an SK3 motorized stage (Marzhauser, Germany). Acquisition and analysis were performed with commercial software (Northern Eclipse, EMPix Imaging Inc., Toronto, Ontario, Canada and Metamorph, Universal Imaging, USA). Figures were processed using PhotoShop 7.0 (Adobe Systems Inc.).

Definition and Quantification of MNI Types

The frequency and neurite composition of MNIs in hippocampal and cortical cultures were determined using $\times 63$ images of neurons immunostained for MAP2 and NFM. Intersections among three dendrites were considered as an MNI of three dendrites, regardless of whether axons were also involved. Only dendrites and axons that reached an intersection point by growing toward it were included in the definition of MNIs. Dendrites or axons arriving at the intersection through fasciculation were excluded (Fig. 1D). MNIs were thus defined as a convergence among three or more neurites, with at least three neurites sharing at least one common pixel. Cell bodies were identified by their MAP2 fluorescence.

For time lapse experiments, one phase contrast image was taken each day. The coordinates of these fields were saved to be returned to successively using a motorized stage. MNIs were identified in a *post hoc* manner; their identity to MNIs from previous days was determined by their position and the surrounding topology of the network.

Definition and Measurement of Clustering of Axonal Varicosities

Images of MAP2 and synaptophysin stained cultures were captured at $\times 63$. Circles of 7.5 µm diameter were centered on MNIs, intersections or single dendrites, as determined by the MAP2 staining. The integrated synaptophysin fluorescence within each circle was measured using a threshold set per image to exclude background staining. Next, the values of all circles in a certain image were normalized by dividing their integrated fluorescence by that of the circle with the highest integrated fluorescence. In this way integrated fluorescence of images from different experiments could be compared. The integrated fluorescence was considered proportional to the local expression of synaptophysin.

FM1-43 Labeling and Measurement

Uptake and secretion of FM1-43 were monitored as described by (Betz *et al.*, 1996). Briefly, cultures maintained for 16–17 days were exposed for 30 s to 15 µM FM1-43 (Molecular Probes) in Tyrode's buffer (in mM: NaCl, 119; KCl, 5; CaCl₂, 4; MgCl₂, 2; glucose, 30; HEPES, 20, pH 7.3), supplemented with 90 mM K⁺ followed by a 3 min wash with Tyrode's buffer at a rate of 1 ml/min. For each cover slip, images of two to four fields randomly selected were obtained under non-saturating conditions, as described above, using a $\times 63$ Plan-Apochromat 1.4 numerical aperture objective (Zeiss). FM1-43 was then secreted in response to an application of 90 mM K⁺ solution in Tyrode's buffer for 30 s, followed by a 3 min wash with Tyrode's buffer at a rate of 1 ml/min. Images of the same fields were obtained, and then immunostained with a combination of anti-MAP2 and anti-NFM antibodies, as described above.

Images acquired after the secretion of FM1-43 were subtracted from those obtained after uptake of FM1-43. The result was used to assess the size of the releasable vesicle pool. These images were analyzed in the same manner as the synaptophysin images described in the previous section.

Boutons were estimated by determining a fluorescence threshold within each circle region (placed as described above). The threshold was used to measure the integrated fluorescence within each object individually, assuming that objects correlated with boutons.

Transfection of Cells

Cultures were transfected for between 5 and 10 days *in vitro* as described previously (Kohrmann *et al.*, 1999). In brief, cells were washed and incubated for 45 min at 37°C with warm MEM (Sigma) and 0.5% glucose. Each coverslip was then incubated for 30–40 min at 37°C with 80 µl of DNA solution until formation of heavy precipitate. The DNA solution comprised: 5 µg DNA (pIRES2-EGFP, Clontech), 250 µl of 250 mM CaCl₂ and 250 µl of BBS (in mM: NaCl, 280; Na₂HPO₄, 1.5; BES, 50, pH 7.1). Finally, cells were washed twice with warm HBS (in mM: NaCl, 135; KCl, 4; Na₂HPO₄, 1; CaCl₂, 2; MgCl₂, 1; glucose, 10; HEPES, 20, pH 7.35) and twice with warm MEM, then returned to their original growth medium. Cells were imaged 5–8 days after transfection.

Cell Labeling for Time Lapse Recordings

Dissociated cells were incubated for 1 h with 100 µg/ml Dil (Molecular Probes) (stock in ethanol) in culture medium at 37°C. Cells were washed of dye residues by sedimentation through 5% BSA in phosphate-buffered saline. The pellet was rinsed with culture medium and cells were plated at a concentration of 2×10^5 cells/ml. The Dil labeled both axons and dendrites in culture.

Results

Formation of MNIs

To study the formation of MNIs we used neuronal cultures, since their neurites are sparse and their wiring is readily monitored. We focused on two culture preparations whose morphological and physiological properties are preserved in culture: the cortex (Dichter, 1978; Gopal and Gross, 1996) and the hippocampal mossy fiber and associational-commissural connections (Johnston *et al.*, 1992; Baranes *et al.*, 1996, 1998).

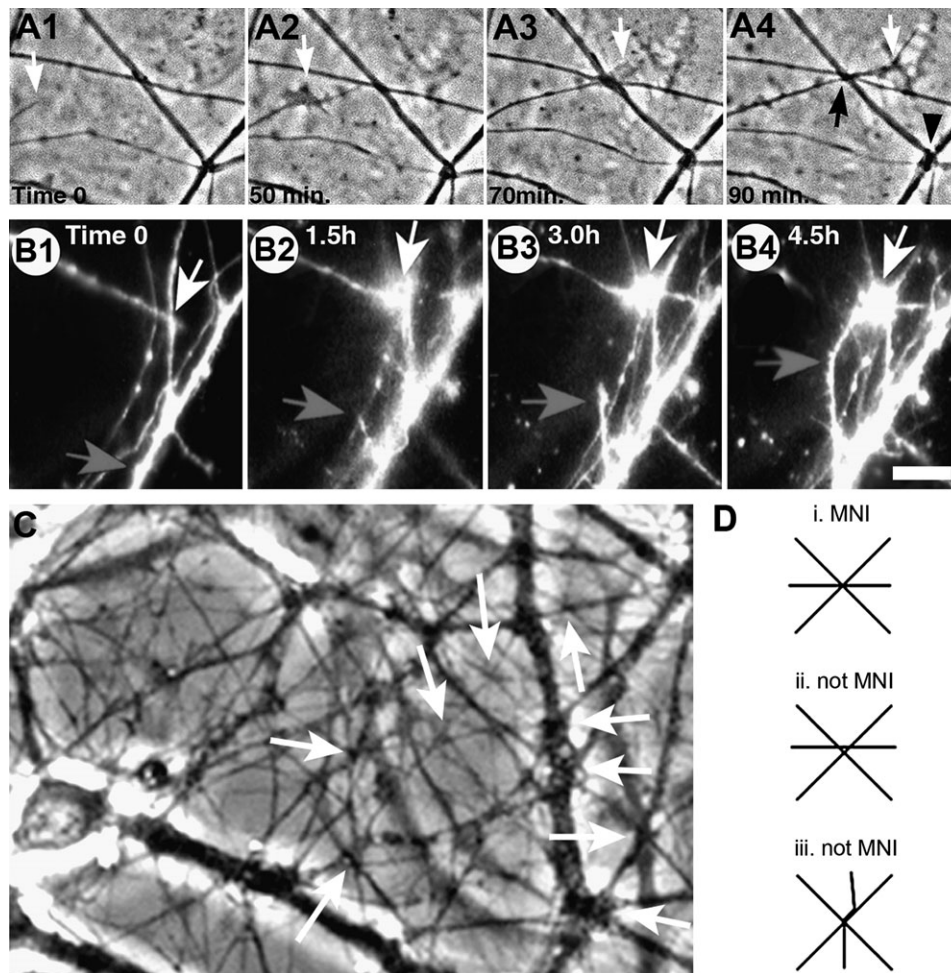


Figure 1. Directed growth of neurites through neurite intersections to form MNIs in 14-day-old hippocampal cultures. (A1–4) Growth of a neurite through a neurite intersection (black arrow in A4), shown by phase-contrast time-lapse microscopy (white arrows indicate the growth cone; arrowhead in A4 indicates a non-MNI intersection). (B1–4) Dil-labeled neurite (bottom arrow) curving (B4) toward a neurite intersection (upper arrow). (C) Representative culture exhibiting a high density of MNIs (arrows). (D) Schematic definition of an MNI, as an intersection of at least three non-fasciculating neurites with at least one common pixel (see Materials and Methods for explanation). Scale bar: A, B, 15 μm ; C, 8 μm .

Neurites of hippocampal neurons grown for 5–7 days *in vitro* (DIV) were initially imaged by phase-contrast microscopy. Neurites growing directly (Fig. 1A1–4) or curving (Fig. 1B1–4) towards neurite intersections were easily detected during 90 min time-lapse recordings. Such directed growth could begin dozens of microns away from the intersection (data not shown). The following sequence of events led to formation of MNIs: (i) once the growth cone approached the intersection, a filopodium made contact with the intersection or with one of the dendrites near the intersection and slid toward the intersection (Fig. 1A2); (ii) the growth cone followed the filopodium to make contact with the intersection (Fig. 1A3); and (iii) the growth cone crossed the intersection (Fig. 1A4). Eventually, the neurite intersection included three or more neurites (Fig. 1C). MNIs were defined strictly as intersections with at least three neurites sharing at least one common pixel (Fig. 1Di). Intersections at which one of the neurites did not traverse the intersection (Fig. 1Dii) or at which neurites reached the intersection through fasciculation with another neurite (Fig. 1Diii) were excluded (see also methods). MNIs were abundant and included both thin (0.5–1.5 μm) and thick (1.5–4 μm) neurites (Fig. 1C). The MNIs

were neuron specific and did not include astrocytic processes, as revealed by immunostaining with anti-glial fibrillary acidic protein (not shown).

MNI Stability

In order to determine the structural stability of MNIs, we followed individual MNIs in 2- to 3-week-old cultures by phase contrast imaging, once a day for up to 6 days (Fig. 2A). Intersections between two neurites were not analyzed because their separation could not be monitored. Intersections suspected to include glial processes were also discarded from analysis. Individual MNIs had varying longevities; for simplicity, we defined MNIs lasting <3 days as short-lived and those lasting ≥ 3 days as long-lived (Fig. 2B). Many of the MNIs were stable throughout the 6 days of the experiment. The median longevity of MNIs in hippocampal cultures was ~ 3 days, with $51.5 \pm 4\%$ short-lived and $48.5 \pm 10.1\%$ long-lived ($n = 48$ MNIs on the first day from four fields from four cultures). In cortical cultures MNIs exhibited similar stability, having $51.4 \pm 3.5\%$ short-lived MNIs and $48.4 \pm 2.8\%$ long-lived MNIs, with $21.6 \pm 6.4\%$ lasting >5 days ($n = 4$ fields with 58 MNIs on the first day, from four cultures). The number of stable MNIs, from both culture types

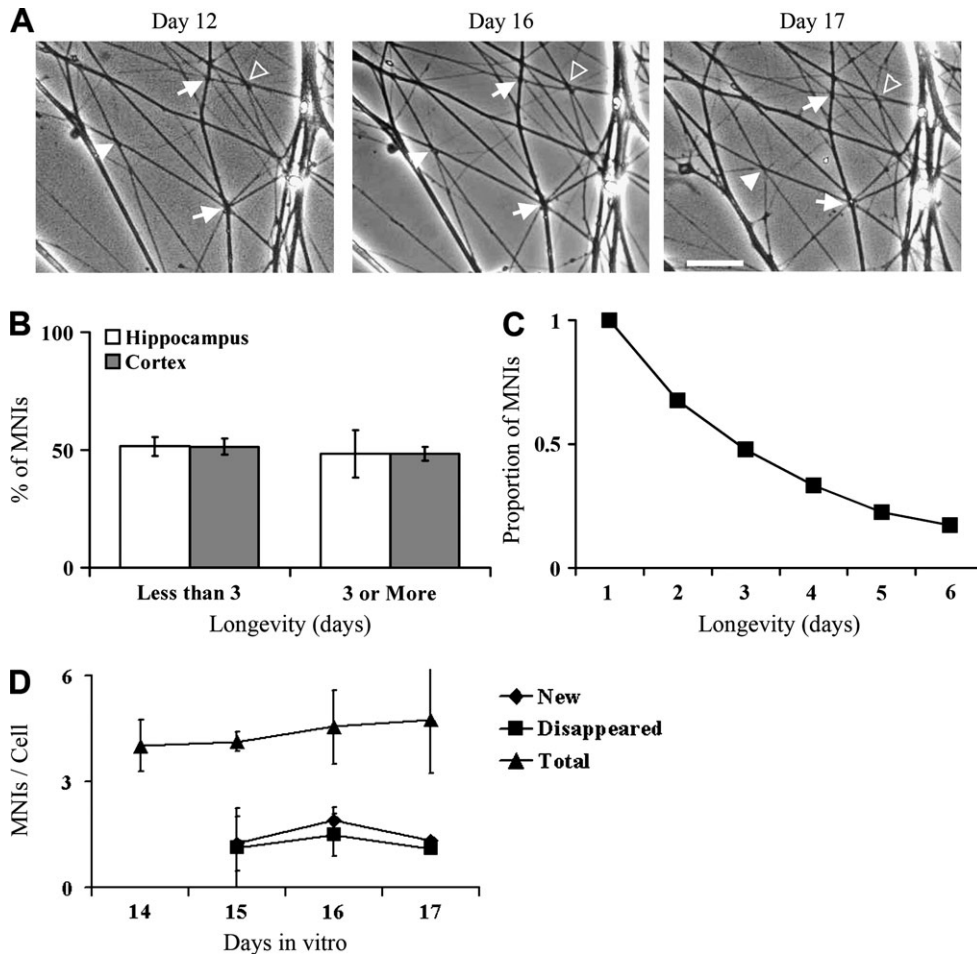


Figure 2. MNIs in hippocampal and cortical cultures are stable, lasting for days. (A) A representative field from a time lapse experiment done in a cortical culture showing stable (arrows), new (full arrowhead) and unstable (empty arrowhead) MNIs. Note the significant modifications of neurites in the left and right parts of the images. (B) Longevity of nearly 50% of MNIs is >3 days in both hippocampal and cortical cultures [$n = 48$ MNIs (hippocampus), 58 MNIs (cortex), 16 fields from four cultures per tissue]. (C) The distribution of MNI longevities. Note that around 15% of MNIs stabilize (pooled data of all MNIs in B). (D) Rates of MNI formation and dissolution are approximately equal, leading to a fixed density of MNIs (analysis of the same MNIs as in B). Scale bar: 10 μ m.

stabilizes at ~15%, which survive for 6 days or more (Fig. 2C). The results obtained here provide an underestimate of the real lifespan of MNIs, since the observed MNIs were formed at variable times prior to the experiment. We also found that rates of MNI formation and dissolution were approximately equal and constant, keeping the overall density of MNIs per cell constant during the entire experiment (Fig. 2D). These results demonstrate that neurites in culture form stable contacts at MNIs, lasting many days.

Frequency of MNIs in Culture versus in Simulations of Randomly Reconstructed Networks

Intersections and MNIs made by dendrites (identified by anti-MAP2) were easier to analyze than those involving axons due to their lower degree of fasciculation. MNIs composed of multiple dendrites could easily be detected (Fig. 3A,B) and accounted for ~10% of total dendritic intersections (Fig. 3C). Over 70% of these MNIs were composed of three dendrites, as in Figure 3B (equivalent to six dendritic segments in the inset of Fig. 3C), whereas the other MNIs included more dendrites (Fig. 3C, inset). Often, single dendritic branches were involved in more than one MNI (Fig. 3A; see also Fig. 3F).

To determine whether MNIs occur more frequently than expected from random superposition of dendrites, we built the expected random frequency of occurrence on the basis of random reconstruction of dendritic networks. We randomly reconstructed 2-D images of dendritic networks by bootstrapping whole dendritic trees visualized by MAP2 immunofluorescence. Each selected dendritic tree was randomly positioned and rotated in the field. We then proceeded to add more cells until the field was populated with the same cell density as that observed in culture (Fig. 3D). The number per cell of MNIs composed of three or more dendrites (six or more dendritic segments) was 3.96-fold higher ($P < 0.001$, t -test) in the hippocampal culture than that in the simulation (Fig. 3E) (1.07 ± 0.32 versus 0.27 ± 0.03 , culture $n = 5$ fields, 90 cells; simulation $n = 5$ simulations, 126 cells). Moreover, in the culture a dendrite could often be involved in more than one MNI (Fig. 3A,F), while in the simulation this behavior was fourfold less frequent (Fig. 3F) ($P < 0.001$, t -test; 32% versus 12% for dendrites with two MNIs and 11% versus none, for dendrites with more than two MNIs). Thus, the frequency of dendritic MNIs in culture is higher than expected from arbitrary dendritic distribution and suggests that dendritic MNIs are formed non-randomly by direct growth of neurites toward neurite intersections.

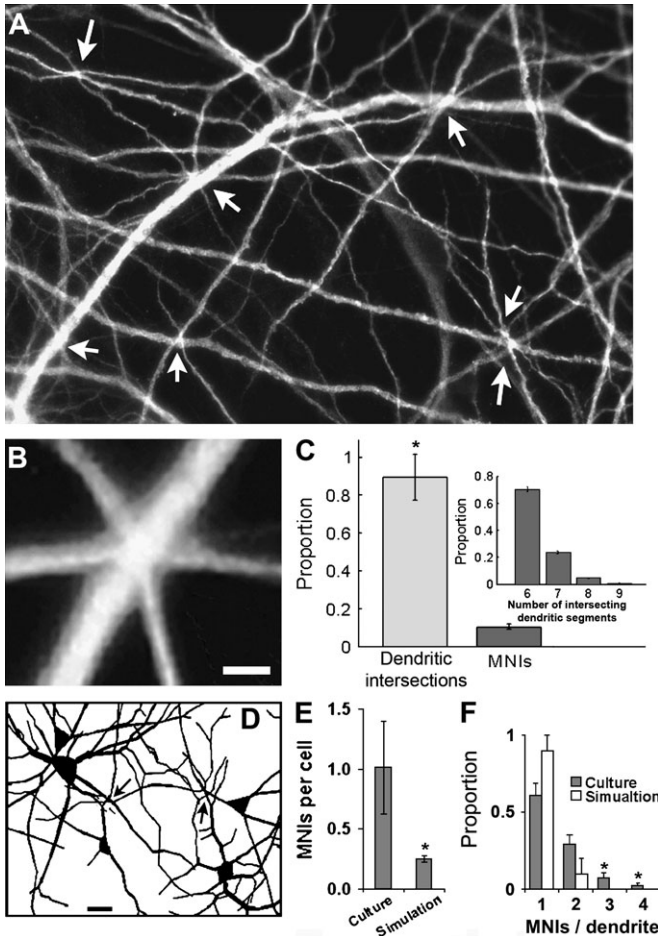


Figure 3. MNIs composed of dendrites are more frequent in hippocampal cultures than in simulations of random dendritic distribution. (A) Dendrites (identified with anti-MAP2) forming MNIs (arrows) in a 12-day-old culture; ~50% of the dendrites in this field are involved in MNIs. (B) An MNI made by three dendrites sharing common pixels. (C) Proportion of intersections between two dendrites (four dendritic segments) versus MNIs with three or more dendrites (six or more dendritic segments). Inset: proportion of MNIs as a function of the number of intersecting dendritic segments. (D) Computer simulation of random cell positioning and orientation of real neurons and their dendrites; all MNIs are indicated by arrows. (E) The observed MNI density per field is nearly four times greater than the expected density computed from random reconstructions (error bars represent SD, $P < 0.001$, t -test, $n = 90$ cells from five cultures and 126 cells from five simulations). (F) Among MNI bearing dendrites, there is a threefold higher chance in culture than in simulation that the dendrite bears a second MNI. In culture 7% of MNI bearing dendrites have three MNIs and 2% have four MNIs, while in simulations we found no dendrites with >2 MNIs (error bars represent SEM, $P < 0.01$ by paired t -test for three or four MNIs per dendrite. $n = 5$ simulations versus 72 dendrites in 10 fields from four cultures). Scale bar: A, 15 μm ; B, 2 μm ; D, 30 μm .

High Frequency of Dendritic and Axonal Involvement in MNIs

We then extended our analysis to include MNIs that involved intersections between dendrites (identified by their MAP2 immunofluorescence) and axons (identified by their NFM immunofluorescence). An MNI could be formed by a single axon or by a fascicle of axons crossing either pre-existing intersections between two dendrites (Fig. 4A) or pre-existing intersections between an axon and a dendrite (Fig. 4B). The density of axon-including MNIs/cell in hippocampal cultures increased as the culture matured (Fig. 4C), from 2.26 ± 0.81 at 7 days *in vitro* (DIV), to 5.2 ± 0.52 at 12–14 DIV and 6.16 ± 2.14 at 18–21 DIV [$P < 0.05$, one-way analysis of variance (ANOVA),

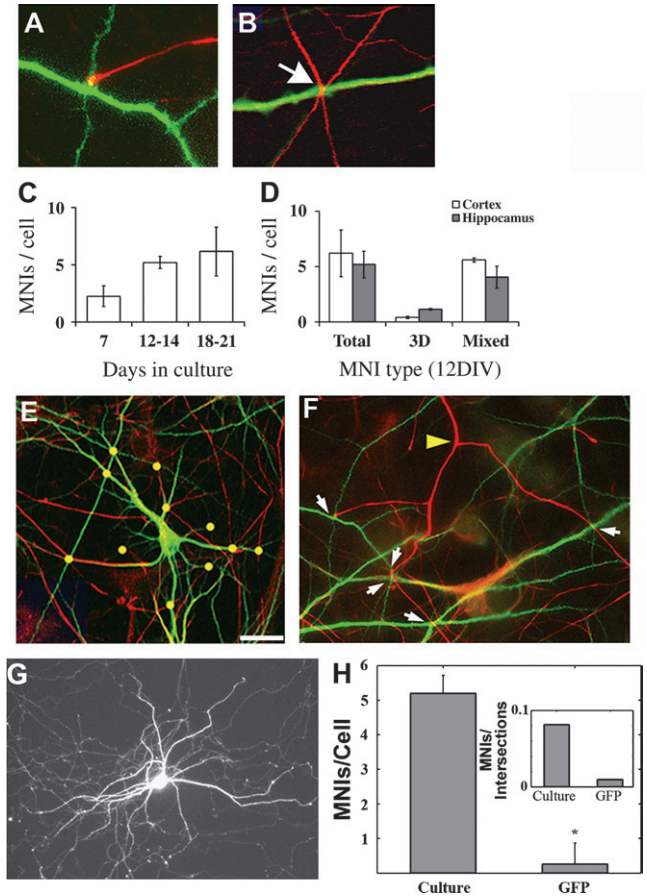


Figure 4. MNIs are formed by axons and dendrites from different cells. Axons are shown in red (anti-NFM) and dendrites in green (anti-MAP2). (A) An axonal growth cone growing directly toward a dendritic intersection. (B) An MNI between two axons and a single dendrite. (C) Density of MNIs increases with culture maturation (D), due mainly to an increase in the number of MNIs that include axons ($n = 150$ – 200 MNIs from 7–10 fields in 3–4 experiments for each age). (E) A cell whose entire dendritic tree is involved in MNIs (yellow spots). (F) An axon or fascicle of axons (yellow arrowhead) growing toward several dendritic intersections, making five MNIs (arrows), suggesting guided axonal growth toward neurite intersections. (G) Very few MNIs are formed among the neurites of individual neurons, as visualized by GFP-expressing neurons. (H) Density of intercellular versus intracellular MNIs, visualized by transfection with GFP [error bars represent SD, $P < 0.001$ by t -test, n (GFP) = 26 cells from five cultures, n (culture) = 28 fields from eight cultures]. Scale bar: A, B, 10 μm ; E, 30 μm ; F, 40 μm ; G, 60 μm .

$n = 150$ – 200 MNIs from 7–10 fields in 3–4 experiments for each age]. This increase was mainly due to axonal growth toward neurite intersections. This is deduced from finding that the density of MNIs composed of three or more dendrites did not change significantly from 7 to 12 DIV, whereas the density of MNIs including one or two dendrites intersecting with axons increased 4.9-fold. Eventually, at the age of 12–14 DIV, 80% (cortical cultures) to 90% (hippocampal cultures) of the MNIs included one or two dendrites intersecting with axons, whereas the rest included three dendrites or more with or without crossing axons (Fig. 4D). The number of dendrites involved in MNIs also increased with culture maturation. While only one-third of dendrites were involved in MNIs of all types during the first week of culture, at 12 and 21 DIV this proportion increased to ~50 and 80%, respectively, until all the dendritic branches of a large portion of the neurons were involved in MNIs (Fig. 4E). Similarly, axonal involvement in MNIs was high, as observed by frequent involvement of single axons or fascicles of axons in

a number of MNIs (Fig. 4F). These results reveal a high frequency of axon and dendrite involvement in MNIs, suggesting MNI formation to be a pivotal factor in controlling arbor shapes and wiring of neurites.

MNIs Are Formed Specifically among Neurites of Different Cells

When dendritic trees of individual neurons in 18-day-old cultures were visualized by transfection with GFP (Fig. 4G), almost no MNIs were detected among the neurites of individual cells (Fig. 4H). The density of MNIs formed from the neurites of a single cell was 0.3 ± 0.6 MNIs/cell (mean \pm SD, $n = 26$ cells from five cultures). In contrast, when dendritic trees of all the neurons in fields of the same 18-day-old cultures were visualized by MAP2 immunofluorescence, the density of MNIs was >17-fold higher (5.3 ± 0.9 MNIs/cell, $n = 28$ fields, eight cultures, $P < 0.001$ by *t*-test, Fig. 4H). In addition, the dendritic trees of different cells have varying sizes and branching orders, which may affect the MNI/cell ratio. We accounted for this by using the ratio of MNIs to intersections for each cell. This ratio was eightfold higher in MNIs formed among neurites of different cells (0.08 ± 0.06) than in MNIs formed among the neurites of single cells (0.01 ± 0.02) [Fig. 4H inset, $P < 0.001$ by *t*-test, n (GFP) = 26 cells from five cultures, n (culture) = 28 fields from eight cultures]. Thus, MNIs are preferably formed among neurites of different cells and are rare among neurites of a single cell.

Clustering of Axonal Varicosities at MNIs

During the second and third weeks *in vitro*, many of the axonal varicosities assembled into clusters at intersections between two or more dendrites (Fig. 5A,B). To quantify the level of clustering, we measured the integrated synaptophysin fluorescence along single dendrites, at two dendrite intersections and at three dendrite MNIs, within a circle 7.5 μ m in diameter centered on the contact site, and normalized the measurements from each image by the circle with highest integrated fluorescence. Normalized integrated fluorescence of synaptophysin per dendrite was higher in MNIs than in intersections or non-intersecting dendritic regions (Fig. 5C). In cortical cultures the normalized integrated synaptophysin fluorescence per dendrite (arbitrary units) was 0.25 ± 0.03 in non-intersecting dendritic regions, 0.27 ± 0.03 at two dendrite intersections and 0.43 ± 0.04 at three dendrite MNIs ($P < 0.01$, one-way ANOVA, $n = 40$ fields from three cultures). In hippocampal cultures there was similar enrichment (in arbitrary units), of 0.07 ± 0.03 , 0.21 ± 0.03 and 0.47 ± 0.03 for single dendrites, intersections and MNIs, respectively ($P < 0.001$, one-way ANOVA, $n = 18$ fields from 12 cultures). These results show that the synaptophysin content of axonal varicosities was elevated at MNIs among dendrites compared with that found in varicosities elsewhere, suggesting either clustering or enrichment of these varicosities in MNIs.

Enhancement of Synaptic Secretion at MNIs

To investigate whether the clustered axonal varicosities are functional presynaptic sites and to compare their release capability to that of terminals located out of the MNIs, synaptic release was evaluated by using the synaptic vesicle recycling marker FM1-43 (Betz WJ *et al.*, 1996). We found FM1-43 turnover at MNIs, suggesting that the clustered synaptophysin puncta formed active axonal terminals. Moreover, the location of many of these terminals on dendrites strengthens the pos-

sibility that they are active presynaptic sites. The level of FM1-43 turnover was higher within MNIs than in non-intersecting dendritic regions or at two dendrite intersections (Fig. 5D,E). Furthermore, the integrated fluorescence of secreted FM1-43 per estimated bouton was 34-fold higher in the cortex ($P < 0.001$ by one-way ANOVA) and 75-fold higher in the hippocampus ($P < 0.001$ by one-way ANOVA) in MNIs than in non-intersecting dendritic regions, while intersections were similar to non-intersecting dendritic regions (Fig. 5F). In cortical cultures, the fold increase of integrated FM1-43 fluorescence relative to nonintersecting dendritic regions, was as follows: nonintersecting regions, 1.0 ± 3.8 ; two dendrite intersections, 11.7 ± 9.8 ; and three dendrite MNIs, 70.2 ± 19.8 ($P < 0.001$, one-way ANOVA, $n = 11$ fields from three experiments). A similar increase was found in hippocampal cultures, with 1.0 ± 2.0 for nonintersecting regions, 8.2 ± 4.6 for intersections and 74.9 ± 9.7 for MNIs ($P < 0.001$, one-way ANOVA, $n = 24$ fields from 12 cultures).

Moreover, the FM1-43 turnover, normalized for the number of intersecting dendrites, also increased (Fig. 5G). In cortical cultures, the normalized integrated FM1-43 fluorescence per dendrite (in arbitrary units) was 0.04 ± 0.03 , 0.18 ± 0.07 and 0.39 ± 0.03 for single dendrites, intersections and MNIs, respectively ($P < 0.001$, one-way ANOVA, $n = 11$ fields from three experiments). Hippocampal cultures exhibited virtually the same relation, in arbitrary units, 0.11 ± 0.04 for nonintersecting dendrites, 0.08 ± 0.04 at intersections and 0.58 ± 0.05 at MNIs ($P < 0.001$, one-way ANOVA, $n = 24$ fields from 12 experiments). These results indicate that the axonal varicosities enriched at MNIs are active presynaptic sites whose secretion level is enhanced with the number of intersecting dendrites.

Synaptic Activity Elevates MNI Density and Clustering of Axonal Varicosities at MNIs in Hippocampal Cultures

MNI density in cells exposed to CNQX, an antagonist of AMPA-type glutamate receptors, was lower than that in untreated cells (Fig. 6A) (59.6 ± 11.9 % MNIs/cell of control, $n = 30$ fields from three experiments each per condition). Treatment with AP-5, an antagonist of the NMDA-type glutamate receptor, caused an insignificant increase in MNI density, whereas exposure of the cultures to TTX, a blocker of presynaptic release, resulted in an insignificant decrease of MNI density. Thus, the results indicate that synaptic activity through AMPA receptors is necessary for formation or maintenance of MNIs.

Similarly, clustering of axonal varicosities at MNIs was sensitive to inhibitors of synaptic activity. The integrated fluorescence of synaptophysin puncta in MNIs was reduced upon inhibition of synaptic activity (Fig. 6B). TTX caused a reduction of integrated synaptophysin fluorescence to $50.8 \pm 4\%$ of the control ($P = 0.02$, *t*-test), and AP-5 reduced it to $38.2 \pm 4\%$ of the control ($P = 0.002$, *t*-test), whereas CNQX lacked an effect with $102 \pm 6.8\%$ of the control ($n = 35$ MNIs from 14 fields for each pharmacological condition). These results indicate that the synaptophysin content and clustering of axonal terminals at MNIs are up-regulated by synaptic activity through NMDA receptors.

Discussion

This study describes the formation of MNIs in cultures of hippocampal and cortical neurons and their role in clustering and secretion capability of axonal terminals. MNIs are formed

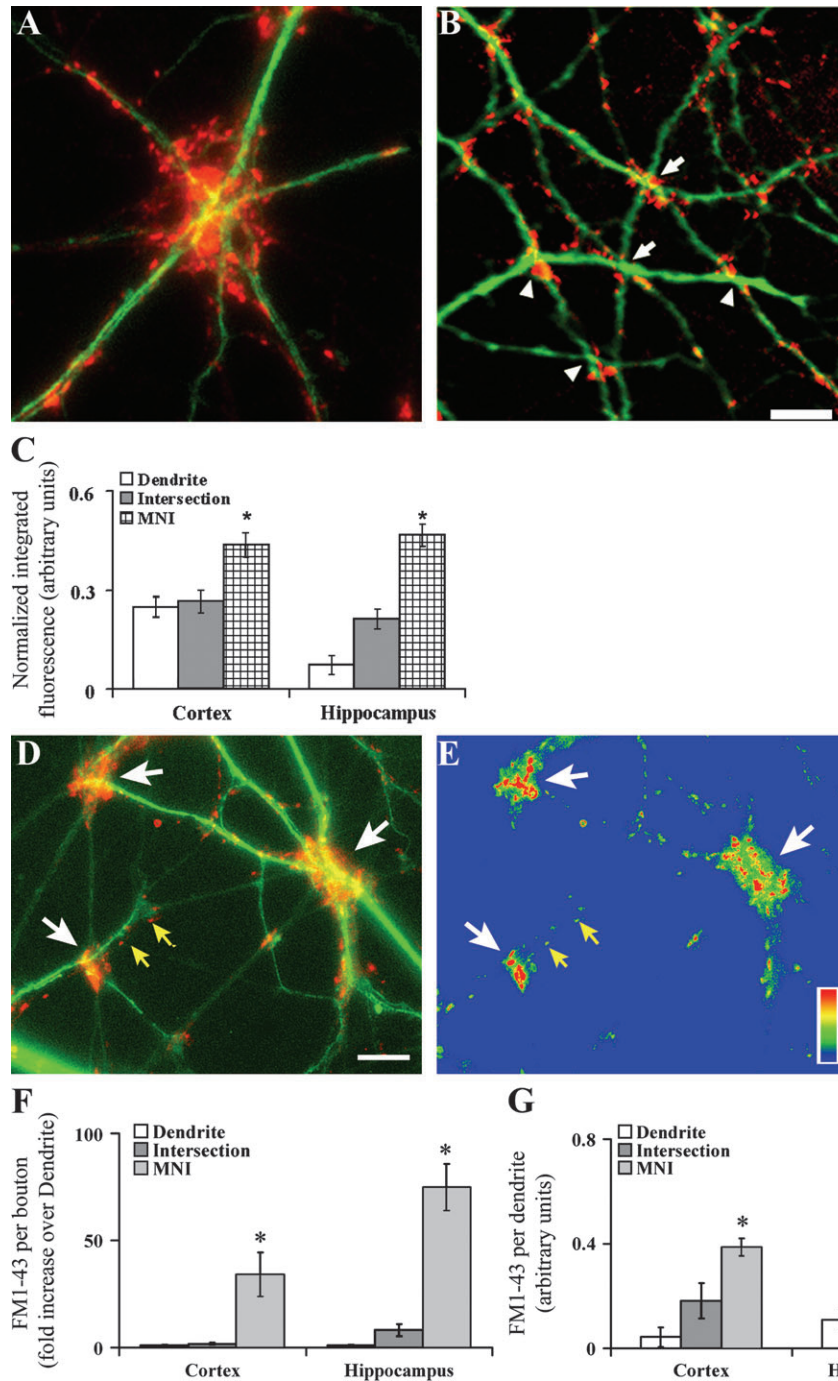


Figure 5. Activity-regulated clustering of axonal varicosities at MNIs in hippocampal and cortical cultures. (A) A cluster of axonal varicosities (red puncta, anti-synaptophysin) on MNIs between seven dendritic segments (green, anti-MAP2). Note that the density and size of varicosities in these clusters are higher than those in non-intersecting regions along the dendrites. (B) A field showing 70% of the dendritic intersections (arrowheads) and 100% of dendritic MNIs (arrows) associated with a cluster of axonal varicosities with a density higher than that found in non-intersecting dendritic areas. (C) Integrated synaptophysin fluorescence (within a circle of 7.5 μm centered on the contact site) normalized per number of dendrites [error bars represent SEM, $P < 0.001$ by one-way ANOVA, n (cortex) = 40 fields from three cultures, n (hippocampus) = 18 fields from 12 cultures]. Varicosities at MNIs have higher synaptic release than varicosities elsewhere. (D) Dendritic MNIs (white arrows) associated with clusters of axonal release sites. Shown is the net release (uptake image minus release image) of FM1-43 (red) overlaid on the dendritic image (green). (E) Color coding of (D) showing that the secretion level is stronger in MNIs (white arrows) than elsewhere (yellow arrows). (F) The integrated fluorescence of FM1-43 secretion per estimated bouton increases in MNIs over intersections and non-intersecting dendritic regions in cortical and hippocampal cultures (error bars represent SEM, $P < 0.001$ by one-way ANOVA). (G) The normalized level of FM1-43 secretion per dendrite also increases in cortical and hippocampal cultures [error bars represent SEM, $P < 0.001$ by one-way ANOVA, n (cortex) = 11 fields from three experiments, n (hippocampus) = 24 fields from 12 cultures]. Scale bar: A, 5 μm ; B, 12 μm ; D, E, 8 μm .

by directed growth of axons and dendrites towards neurite intersections, and their development is up regulated by the activity of AMPA receptors. The density of axonal varicosities and their release capability are increased at MNIs compared

with varicosities elsewhere, and this is regulated by synaptic activity. These results show that neurite convergence into MNIs is an activity-regulated wiring behavior that links neurite morphology with clustering and strengthening of

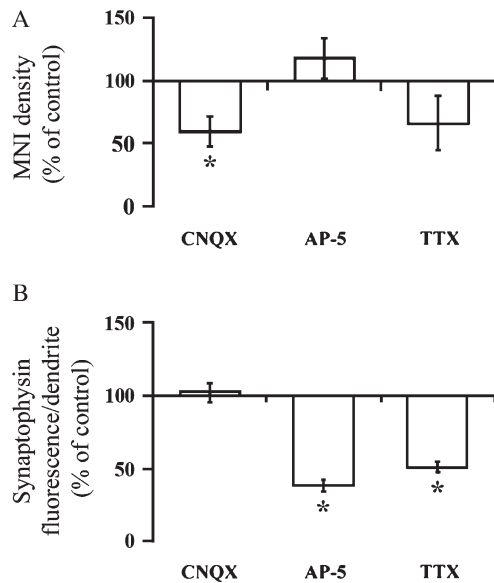


Figure 6. Activity regulates MNI density and clustering of axonal varicosities at MNIs in hippocampal cultures. (A) MNI density in the presence of activity inhibitors. Significant inhibitory effect is observed only with blockade of AMPA receptors with CNQX (error bars represent SEM, $P < 0.05$ by one-way ANOVA). (B) Inhibition of synaptic activity by TTX and AP-5 reduced the fluorescence of synaptophysin in MNIs. Presented is integrated synaptophysin fluorescence per MNI as percent of control (error bars represent SEM, $P = 0.02$, t -test for TTX and $P = 0.002$, t -test for AP-5).

presynaptic sites, a role which may serve in synaptic plasticity.

Our results indicate that the properties of MNIs and their effect on axonal terminal clustering and secretion are similar in hippocampal and cortical cultures. Both cultures had similar frequencies and longevities (Fig. 2B,D) of MNIs, and similar proportions of the different MNI types (Fig. 4C,D), yet the cortical cultures had greater axonal length than the hippocampal cultures (not shown), and therefore had fewer MNIs per axon. So, while the involvement of dendritic branches in MNIs is extensive and similar between the two cell types, the extent of axonal involvement is different. This may explain the more clustered distribution of mossy fiber pre-synaptic terminals in the hippocampus than in the cortex *in vivo* and *in vitro* (Kavalali *et al.*, 1999). Formation of MNIs and synaptic clustering therein can thus be seen to be a general mechanism working to varying extents in diverse neuronal types, affecting their morphology, wiring and activity.

Potential Mechanisms for the Formation of MNIs

An optional mechanism for MNI formation is attraction of neurite growth along gradients of attractants originating from sites of neurite intersections. As mentioned in the introduction, neurite-neurite contacts are enriched with trans-Golgi vesicles (Sytnyk *et al.*, 2002). Clustering of these exocytotic vesicles at intersections can produce an attractant gradient. However, such a mechanism implies that every intersection would become an MNI, whereas our results show that MNIs comprise only 10% of intersections (Fig. 3C). We offer two possible explanations for this discrepancy: (i) While growing towards intersections, neurites cross other neurites, forming new intersections and lowering the MNI/ intersection ratio. (ii) Assuming the majority of neurite intersections form attractant gradients of various strengths in culture, growing neurites are exposed to a mixture of overlapping gradients and miss

intersections with relatively weak gradients. Indeed, we have occasionally encountered neurites growing toward distant intersections, missing closer ones.

Growth cones approaching intersections by an attraction mechanism should stop once reaching the gradient peak, at or near the intersection, yet growth cones clearly cross intersections (Fig. 1A1-4). This finding can be explained by attraction of growth cones crossing specific intersections by larger gradients originating in other intersections. Alternatively, switches in growth cone responsiveness to a gradient, from attraction to repulsion or vice versa, is common (Giger and Kolodkin, 2001).

Mechanisms other than gradients of attractants are likely to be involved in MNI formation. According to the attractant gradient model of MNI formation, neurites from a single neuron, being closer to each other than to neurites of other neurons, should form MNIs and give dendritic trees a globular shape. Our analysis clearly demonstrated that dendritic trees in culture are highly elaborate (Fig. 4F) and that MNIs among dendrites of the same neuron are rare (Fig. 4G). Thus, it is realistic to postulate that MNI formation is a combination of attraction by intersections and intrinsic properties of dendrites, which restrict convergence of neurites of the same cell. This implies the ability for self versus target recognition in the MNI-forming dendrites. This ability could possibly be imparted by involvement of adhesion molecules the likes of protocadherins or IgCAMs in stabilization of cell-cell adhesion contacts at MNIs. These protein families of adhesion molecules exhibit a large variety of homophilic and heterophilic interactions (Kamiguchi and Lemmon, 2000; Hilschmann *et al.*, 2001), allowing for such self and target recognition.

Activity-dependent and -independent Mechanisms of MNI Formation

MNI density is down-regulated upon blockade of AMPA receptors (Fig. 6A). However, the blockade caused only a partial inhibition of MNI formation and not a complete arrest, indicating that AMPA receptors play a regulatory rather than inductive role in MNI formation. Moreover, we detected MNIs in 3-day-old cultures (data not shown) prior to the onset of synaptic activity (Lopez-Garcia *et al.*, 1996). These results suggest that the initial morphology of the neuronal network in culture develops independently of synaptic activity; yet synaptic activity modifies the architecture of the network by enhancing neurite convergence to MNIs. This scenario fits well with the two-stage mechanism of dendritic development in the brain: dendrites are programmed to initially ramify in the absence of synaptic activity, and later on the activity patterns and stabilizes the dendritic trees (Jefferis *et al.*, 2004).

Possible Mechanisms for Synaptic Clustering at MNIs

Several explanations are possible for the higher density and secretion level of axonal terminals at MNIs: (i) a high degree of axonal crossing at MNIs; (ii) enhanced synaptogenesis; or (iii) grouping of pre-existing axonal varicosities. We indeed found many of the enriched MNIs crossed by axons, yet we also found MNIs crossed by single axons to be enriched. It is important to note here that axons fasciculating along the intersecting dendrites also reach the MNIs. This produces an area at or near the center of the MNI, with a higher density of axonal terminals than elsewhere along the intersecting dendrites. Activity of these initial terminals is likely to produce

a glutamate gradient, which is known to attract axons (Zheng *et al.*, 1994; Ruthazer and Cline, 2004). In addition, glutamate gradients increase synaptogenesis (Zheng *et al.*, 1994; Ruthazer and Cline, 2004), which may further increase the density of axonal terminals at the MNIs, above that reached by convergence of axons. In addition, grouping of pre-existing terminals is also possible. Kavalali *et al.* (1999) found that the emergence of synaptic clusters in cultures of the mossy fiber pathway was preceded by a more subtle but highly significant narrowing of the distance between individual neighbouring boutons. Hence, the results point to the high likelihood that formation of clusters of axonal terminals at MNIs is a combination of enhanced axonal convergence and synaptogenesis as well as grouping of pre-existing terminals.

A Role for MNIs in Morphology and Activity of Neuronal Networks

MNIs are expected to affect the morphology and physiology of neuronal networks as follows: (i) the growth of dendritic branches toward intersections shapes dendritic trees by affecting the growth direction and branch length (Fig. 4F). From the second week in culture on, most dendritic branches were involved in at least one MNI (not shown) and many were involved in more than one MNI (Fig. 3F), suggesting that MNIs are frequent enough to affect the entire dendritic network. In turn, the shape of dendritic trees affects dendritic integration, as mentioned in the introduction, thereby influencing the activity of the entire neuronal network. (ii) Dendrites at intersections are selected as axonal targets by the non-random growth of axons or bundles of axons directly towards neurite intersections. Moreover, crossing axons innervate the target dendrites at this specific location, the intersection. The high frequency of axonal convergence into intersections may have a strong influence on the pattern of inputs along dendritic trees, as shown in Figure 4E. (iii) The increased proximity and secretion levels among the clustered synaptic connections at MNIs may reduce the amplitude but increase the frequency of their firing (Liu and Tsien, 1995) and promote their summation (Polsky *et al.*, 2004) compared with more separated synaptic connections. Hence, the patterns of morphology and activity of neuronal networks may be designed by the extent to which neurites converge to form MNIs.

The fact that synaptic activity increases both MNI formation and the secretion capability of axonal terminals at MNIs suggests that neurite wiring through MNIs mediates activity-dependent synaptic strengthening. Hence, information entering a neuronal network can be consolidated by inducing convergence of axons and dendrites into MNIs, resulting in clustering and strengthening of specific sets of synaptic connections.

Notes

We would like to thank Dr John J.M. Bergeron for helpful discussions, for his support and for reading the manuscript. We thank Drs Tim Kennedy, Wayne Sossin, Angel Alonso and Peter McPherson of the Montreal Neurological Institute and Dr Yael Amitai of Ben-Gurion University for critical reading of the manuscript. This work was supported by grants from the Canada Foundation of Innovation and the Toman fellowship, Ben-Gurion University of the Negev.

Address correspondence to Dr Danny Baranes, Department of Life Sciences, Ben-Gurion University of the Negev, Beer-Sheva 84105, Israel. Email: dbaranes@bgumail.bgu.ac.il.

References

- Baranes D, LopezGarcia JC, Chen M, Bailey CH, Kandel ER (1996) Reconstitution of the hippocampal mossy fiber and associational-commissural pathways in a novel dissociated cell culture system. *Proc Natl Acad Sci USA* 93:4706–4711.
- Baranes D, Lederfein D, Huang YY, Chen M, Bailey CH, Kandel ER (1998) Tissue plasminogen activator contributes to the late phase of LTP and to synaptic growth in the hippocampal mossy fiber pathway. *Neuron* 21:813–825.
- Betz WJ, Mao F, Smith CB (1996) Imaging exocytosis and endocytosis. *Curr Opin Neurobiol* 6:365–371.
- Buzsaki G, Geisler C, Henze DA, Wang XJ (2004) Interneuron diversity series: circuit complexity and axon wiring economy of cortical interneurons. *Trends Neurosci* 27:186–193.
- da F. Costa L, Barbosa MS, Coupez V (2004) A direct approach to neuronal connectivity. *Physica A: Statist Mech Appl* 341:618–628.
- Dichter MA (1978) Rat cortical neurons in cell culture: culture methods, cell morphology, electrophysiology, and synapse formation. *Brain Res* 149:279–293.
- Fletcher TL, De Camilli P, Banker G (1994) Synaptogenesis in hippocampal cultures: evidence indicating that axons and dendrites become competent to form synapses at different stages of neuronal development. *J Neurosci* 14:6695–6706.
- Giger RJ, Kolodkin AL (2001) Silencing the siren: guidance cue hierarchies at the CNS midline. *Cell* 105:1–4.
- Gopal KV, Gross GW (1996) Auditory cortical neurons *in vitro*: cell culture and multichannel extracellular recording. *Acta Otolaryngol* 116:690–696.
- Hilschmann N, Barnikol HU, Barnikol-Watanabe S, Gotz H, Kratzin H, Thinnies FP (2001) The immunoglobulin-like genetic predetermination of the brain: the protocadherins, blueprint of the neuronal network. *Naturwissenschaften* 88:2–12.
- Jefferis GSXE, Komiyama T, Luo L (2004) NEUROSCIENCE: calcium and CREST for healthy dendrites. *Science* 303:179–181.
- Johnston D, Williams S, Jaffe D, Gray R (1992) NMDA-receptor-independent long-term potentiation. *Annu Rev Physiol* 54:489–505.
- Kamiguchi H, Lemmon V (2000) IgCAMs: bidirectional signals underlying neurite growth. *Curr Opin Cell Biol* 12:598–605.
- Kavalali ET, Klingauf J, Tsien RW (1999) Activity-dependent regulation of synaptic clustering in a hippocampal culture system. *Proc Natl Acad Sci USA* 96:12893–12900.
- Kim S, Chiba A (2004) Dendritic guidance. *Trends Neurosci* 27:194–202.
- Koester SE, O'Leary DD (1992) Functional classes of cortical projection neurons develop dendritic distinctions by class-specific sculpting of an early common pattern. *J Neurosci* 12:1382–1393.
- Kohrmann M, Haubensak W, Hemraj I, Kaether C, Lessmann VJ, Kiebler MA (1999) Fast, convenient, and effective method to transiently transfect primary hippocampal neurons. *J Neurosci Res* 58:831–835.
- Krichmar JL, Nasuto SJ, Scorcioni R, Washington SD, Ascoli GA (2002) Effects of dendritic morphology on CA3 pyramidal cell electrophysiology: a simulation study. *Brain Res* 941:11–28.
- Lago-Fernandes LF, Huerta R, Corbacho F, Siguenza JA (2000) Fast response and temporal coherent oscillations in small-world networks. *Phys Rev Lett* 84:2758–2760.
- Liu G, Tsien RW (1995) Properties of synaptic transmission at single hippocampal synaptic boutons. *Nature* 375:404–408.
- LopezGarcia JC, Arancio O, Kandel ER, Baranes D (1996) A presynaptic locus for long-term potentiation of elementary synaptic transmission at mossy fiber synapses in culture. *Proc Natl Acad Sci USA* 93:4712–4717.
- Mel BW (1993) Synaptic integration in an excitable dendritic tree. *J Neurophysiol* 70:1086–1101.
- Orioli D, Klein R (1997) The Eph receptor family: axonal guidance by contact repulsion. *Trends Genet* 13:354–359.
- Polsky A, Mel BW, Schiller J (2004) Computational subunits in thin dendrites of pyramidal cells. *Nat Neurosci* 7:621–627.
- Ruthazer ES, Cline HT (2004) Insights into activity-dependent map formation from the retinotectal system: a middle-of-the-brain perspective. *J Neurobiol* 59:134–146.

- Sang Q, Tan SS (2003) Contact-associated neurite outgrowth and branching of immature cortical interneurons. *Cereb Cortex* 13: 677-683.
- Schiller J, Major G, Koester HJ, Schiller Y (2000) NMDA spikes in basal dendrites of cortical pyramidal neurons. *Nature* 404:285-289.
- Scott EK, Luo L (2001) How do dendrites take their shape? *Nat Neurosci* 4:359-365.
- Sestan N, Artavanis-Tsakonas S, Rakic P (1999) Contact-dependent inhibition of cortical neurite growth mediated by notch signaling. *Science* 286:741-746.
- Shefi O, Golding I, Segev R, Ben-Yakov E, Ayali A (2002) Morphological characterization of *in vitro* neuronal networks. *Physical Rev E*: 021905.
- Sytnyk V, Leshchyn'ska I, Delling M, Dityateva G, Dityatev A, Schachner M (2002) Neural cell adhesion molecule promotes accumulation of TGN organelles at sites of neuron-to-neuron contacts. *J Cell Biol* 159:649-661.
- Threadgill R, Bobb K, Ghosh A (1997) Regulation of dendritic growth and remodeling by Rho, Rac, and Cdc42. *Neuron* 19: 625-634.
- Van den Pol AN (1980) The hypothalamic suprachiasmatic nucleus of rat: intrinsic anatomy. *J Comp Neurol* 191:661-702.
- Watts DJ, Strogatz SH (1998) Collective dynamics of 'small-world' networks. *Nature* 393:440-442.
- Whitford KL, Marillat V, Stein E, Goodman CS, Tessier-Lavigne M, Chedotal A, Ghosh A (2002) Regulation of cortical dendrite development by Slit-Robo interactions. *Neuron* 33:47-61.
- Zheng JQ, Felder M, Connor JA, Poo MM (1994) Turning of nerve growth cones induced by neurotransmitters. *Nature* 368: 140-144.